Electromagnetic Scattering Properties in a Multilayered Metamaterial Cylinder

Cheng-Wei Qiu [1,2], Hai-Ying Yao [1], # Saïd Zouhdi [2], and Le-Wei Li [1]

[1] Department of Electrical and Computer Engineering, National University of Singapore
Kent Ridge, Singapore 119260, eleyh@nus.edu.sg

[2] Laboratoire de Génie Électrique de Paris, Ecole Supérieure D'Électricité
Gif-Sur-Yvette Cedex, 91192, France, chengwei.qiu@lgep.supelec.fr

Abstract

In this paper, a multilayered cylinder filled with metamaterials is studied. General formulas of electromagnetic fields in each region are derived using the eigenfunction expansion method. For an infinite line source, the image property is observed when the radius of this cylinder is much larger than the wavelength. The distributions of electromagnetic fields are presented when a line source is placed near a two-layered cylinder alternately filled with double negative (DNG) and double positive (DPS) material. The electric field and energy in the presence of a cylinder with very small radius have been investigated.

1. Introduction

In 1968, Veselago theoretically studied wave characteristics in a special medium whose permittivity and permeability are both negative simultaneously [1]. The hypothetical materials are explored systematically until the split-ring resonator (SRR) structure was proposed [2] and experimentally verified [3]. The double negative (DNG) material has shown special optical properties, and could lead to a perfect lens [4]. For EM waves propagating through a stratified DNG medium, reflection and refraction of the waves were formulated by Kong [5]. The objective of this paper is to extend the existing application from planar structures to cylindrical structures, so as to gain more insight into the hybrid effects of metamaterials and cylindrical curvature.

2. Formulations

Consider an N-layered infinitely-long cylinder situated in free space (ε_0, μ_0), as depicted in Fig. 1. In each layer, it is filled with DNG or DPS homogeneous material of different permittivity and permeability. In the following analysis the time dependence, $e^{-j\omega t}$, is suppressed. The permittivity and permeability of material in region f $(f = 1, \cdots N)$ are denoted as follows:

$$\varepsilon_f = u \mid \varepsilon_f \mid, \qquad (1a)$$
$$\mu_f = u \mid \mu_f \mid, \qquad (1b)$$

An incident wave of transverse electric (TE) or transverse magnetic (TM) polarization is assumed to illuminate
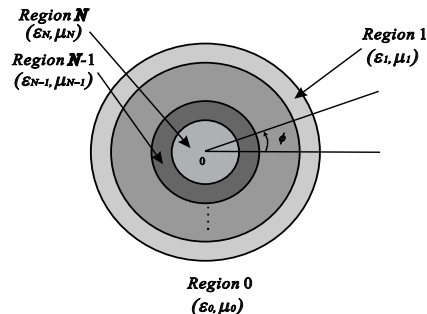

Fig. 1: Geometry of a multilayered cylinder with different materials.

the layered cylinder in free space at an arbitrary oblique angle. In the cylindrical coordinates system, the vector wave functions are given in [6], and rewritten as follows:

$$
\boldsymbol{M}_n^{(p)}(k_z) = \left[\frac{jn}{\rho} B_n^{(p)}(k_\rho\rho)\widehat{\boldsymbol{\rho}} - \frac{dB_n^{(p)}(k_\rho\rho)}{d\rho}\widehat{\boldsymbol{\phi}} \right]
$$
$$
\times e^{j(n\phi + k_z z)}, \qquad (2a)
$$
$$
\boldsymbol{N}_n^{(p)}(k_z) = \frac{e^{j(n\phi + k_z z)}}{k} \left[jk_z \frac{dB_n^{(p)}(k_\rho\rho)}{d\rho}\widehat{\boldsymbol{\rho}} \right.
$$
$$
\left. - \frac{nk_z}{\rho} B_n^{(p)}(k_\rho\rho)\widehat{\boldsymbol{\phi}} + k_\rho^2 B_n^{(p)}(k_\rho\rho)\widehat{\boldsymbol{z}} \right], (2b)
$$

where $B_n^{(p)}(k_\rho\rho)$ represents the cylindrical Bessel functions of order n, the superscript p equals 1 or 3 representing the Bessel function of the first kind and the cylindrical Hankel function of the first kind, and $k^2 = k_\rho^2 + k_z^2$. If the electromagnetic waves are normally incident on the surface, the vector wave functions expressed in (2a) and (2b) can be simplified as:

$$
\boldsymbol{M}_n^{(p)}(k) = \left[\widehat{\boldsymbol{\rho}}\frac{jn}{k\rho}B_n^{(p)}(k\rho) - \widehat{\boldsymbol{\phi}}\frac{dB_n^{(p)}(k\rho)}{kd\rho} \right] e^{jn\phi}, (3a)
$$
$$
\boldsymbol{N}_n^{(p)}(k) = \widehat{\boldsymbol{z}}B_n^{(p)}(k\rho) e^{jn\phi}. \qquad (3b)
$$

By using eigenfunction expansion method, the electric and magnetic fields in the region f $(f = 1, \cdots N-1)$ are

formulated as follows:

$$
\begin{aligned}
\boldsymbol{E}_f &= \sum_{n=0}^{\infty} \left\{ a_{nf} \boldsymbol{N}_n^{(3)}(k_{zf}) + b_{nf} \boldsymbol{M}_n^{(3)}(k_{zf}) \right. \\
&\quad + \left. a'_{nf} \boldsymbol{N}_n^{(1)}(k_{zf}) + b'_{nf} \boldsymbol{M}_n^{(1)}(k_{zf}) \right\}, \quad (4a)
\end{aligned}
$$

$$
\begin{aligned}
\boldsymbol{H}_f &= \frac{k_f}{j\omega u \mid \mu_f \mid} \sum_{n=0}^{\infty} \left\{ a_{nf} \boldsymbol{M}_n^{(3)}(k_{zf}) + b_{nf} \boldsymbol{N}_n^{(3)}(k_{zf}) \right. \\
&\quad + \left. a'_{nf} \boldsymbol{M}_n^{(1)}(k_{zf}) + b'_{nf} \boldsymbol{N}_n^{(1)}(k_{zf}) \right\}. \quad (4b)
\end{aligned}
$$

where a_{nf}, b_{nf}, a'_{nf} and b'_{nf} are the unknown expansion coefficients.

For the out-most region (i.e., Region 0) and the inner-most region (i.e., Region N), the electromagnetic fields can be expanded as:

$$
\begin{aligned}
\boldsymbol{E}_0 &= \boldsymbol{E}^i + \boldsymbol{E}^s \\
&= \boldsymbol{E}^i + \sum_{n=0}^{\infty} \left[a_{n0} \boldsymbol{N}_n^{(3)}(k_{z0}) + b_{n0} \boldsymbol{M}_n^{(3)}(k_{z0}) \right], \quad (5a)
\end{aligned}
$$

$$
\begin{aligned}
\boldsymbol{H}_0 &= \boldsymbol{H}^i + \boldsymbol{H}^s = \boldsymbol{H}^i + \frac{k_0}{j\omega u \mid \mu_0 \mid} \\
&\quad \times \sum_{n=0}^{\infty} \left[a_{n0} \boldsymbol{M}_n^{(3)}(k_{z0}) + b_{n0} \boldsymbol{N}_n^{(3)}(k_{z0}) \right], \quad (5b)
\end{aligned}
$$

and

$$
\boldsymbol{E}_N = \sum_{n=0}^{\infty} \left[a'_{nN} \boldsymbol{N}_n^{(1)}(k_{zN}) + b'_{nN} \boldsymbol{M}_n^{(1)}(k_{zN}) \right], \quad (6a)
$$

$$
\begin{aligned}
\boldsymbol{H}_N &= \frac{k_N}{j\omega u \mid \mu_N \mid} \sum_{n=0}^{\infty} \left[a'_{nN} \boldsymbol{M}_n^{(1)}(k_{zN}) \right. \\
&\quad + \left. b'_{nN} \boldsymbol{N}_n^{(1)}(k_{zN}) \right]. \quad (6b)
\end{aligned}
$$

For the electromagnetic fields in all the regions, we have the same longitudinal wave vector $\boldsymbol{k}_z$ due to phase matching condition, whereas the radial wave vector $\boldsymbol{k}_{\rho f}$ is discontinuous.

In the above formulas, the expansion coefficients, a_{nf}, b_{nf}, a'_{nf}, and b'_{nf}, can be determined by enforcing the boundary conditions of the tangential electric- and magnetic-field components on the cylindrical interfaces at $\rho = r_f$ (where $f = 0, 1, \cdots, N - 1$):

$$
\widehat{\boldsymbol{\rho}} \times \begin{bmatrix} \boldsymbol{E}_f \\ \boldsymbol{H}_f \end{bmatrix} = \widehat{\boldsymbol{\rho}} \times \begin{bmatrix} \boldsymbol{E}_{f+1} \\ \boldsymbol{H}_{f+1} \end{bmatrix}. \quad (7)
$$

A recursive system for the coefficients can be finally obtained [6]:

$$
C_{f+1} = \boldsymbol{T}_f C_f \quad (8)
$$

where $[C_f]$ is defined by:

$$
C_f = \begin{bmatrix} a_{nf}, & b_{nf}, & a'_{nf}, & b'_{nf} \end{bmatrix}^T \quad (9)
$$

and the transmission matrix in the eigen-expansion domain is given by:

$$
\boldsymbol{T}_f = \boldsymbol{F}_{f+1}^{-1} \boldsymbol{F}_f \quad (10)
$$

and the parameter matrices $\boldsymbol{F}_f$ and $\boldsymbol{F}_{f+1}$ are derived from the boundary conditions. All the scattering coefficients can be determined by the recursive algorithm as in Eq. (8).

For an infinitely long line source placed at (ρ_0, ϕ_0) and parallel to the cylinder, the incident electromagnetic wave can be expressed by

$$
\boldsymbol{E}^i = -\frac{k^2 I}{4\omega \varepsilon_0} \sum_{n=0}^{\infty} (2 - \delta_{n0}) H_n^{(1)}(k\rho_0) \boldsymbol{N}_n^{(1)}(k) e^{-jn\phi_0}, \quad (11a)
$$

$$
\boldsymbol{H}^i = -\frac{kI}{4j} \sum_{n=0}^{\infty} (2 - \delta_{n0}) H_n^{(1)}(k\rho_0) \boldsymbol{M}_n^{(1)}(k) e^{-jn\phi_0}, \quad (11b)
$$

where I stands for the amplitude of electric current.

3. Numerical Results

To verify the correctness of the formulations deduced above, we firstly calculate the distant scattering pattern of a two-layed cylinder filled with different DPS materials and radiated by the parallel line source. The geometry is shown in Fig. 2. The radii of two layers from inside to outside are $a = 0.25\lambda$ and $b = 0.3\lambda$, respectively. The corresponding relative permittivity are $\varepsilon_{r1} = 4.0$, and $\varepsilon_{r2} = 1.0$. The relative permeability of two layers are $\mu_{r1} = \mu_{r2} = 1.0$. The line source is placed at a distance of $\rho_0 = 0.5\lambda$ from the center of the layered cylinder, and an observation angle ϕ_0 of 0 degree. The distant scattering pattern can be obtained by the asymptotic form of large-argument Hankel functions, which is shown in Fig. 3, respectively. For the reference, the integral-equation solutions, which come from [7], are also given. An excellent agreement is observed. This partially verified the correctness of our derived theoretical formulas and the developed codes.
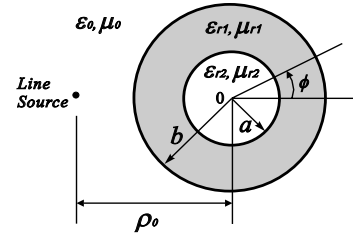

Fig. 2: Geometry of a two-layered cylinder with DPS materials.

First of all, radiation by a line source in the presence of this cylinder is considered. The different radii a are also set. The line source is located at $\rho_1 = 2.3\lambda$ and $\phi_0 = 0$, where ρ_1 is the distance from the surface of the cylinder. Then, the normalized amplitudes of the time-averaged Poynting power, which is denoted by $\langle \boldsymbol{S} \rangle = \frac{1}{2} Re(\boldsymbol{E} \times \boldsymbol{H}^*)$, are shown in Fig. 4-Fig. 5. From
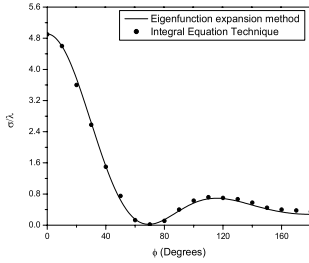
Fig. 3: Scattering pattern of a nearby parallel line source in the presence of a two-layered cylinder with DPS materials.

Fig. 5: Normalized amplitudes of the time-averaged Poynting power for a one-layered cylinder with $(-\varepsilon_0, -\mu_0)$ and $a = 150\lambda$.

Fig. 6: The amplitude of electric field for a one-layered cylinder with $(4\varepsilon_0, \mu_0)$ and $a = 0.05\lambda$.

Fig. 4, we observe that a facula is formed inside the cylinder. The formation of the facula is due to the cylinder with $(-\varepsilon_0, -\mu_0)$ is not a focusing system. This summary point can be verified by using the theory of arbitrary coordinate transformations [8]. According to the theory, if we keep the wave scattering properties unchanged after the geometrical dimension (e.g., the radius) is changed, we have to adjust μ and ε accordingly. When the physical problem is changed from a perfect slab lens to a perfect cylindrical lens, the permittivity and permeability in the lens are required to be a function of position. Hence, the cylinder with $(-\varepsilon_0, -\mu_0)$ cannot focus the light, and it will still reflect waves. However, a phenomenon of focus shown as in Fig. 5 can be obtained when the electric size of calculated problem is far larger than the wavelength.
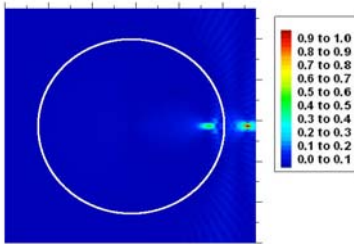

Fig. 4: Normalized amplitudes of the time-averaged Poynting power for a one-layered cylinder with $(-\varepsilon_0, -\mu_0)$ and $a = 8.5\lambda$.

Further, we study the field distribution in the presence of cylinders with small radii. In Fig. 6, the focula denotes the line source which is placed 0.2λ away from the axis of the cylinder (i.e., the origin of the system). It can be seen that the amplitude of the electric field are modified at the position where the cylinder is placed. The wave has been amplified greatly at the position occupied by the cylinder compared to the case that the cylinder is removed. In Fig. 7, the power distribution, between the source and scatterer, gradually converges to the cylinder's position. Afterwards, on the right hand side of the cylinder, there still exists some power. It shows that, on the right hand side, the original power distribution without the presence
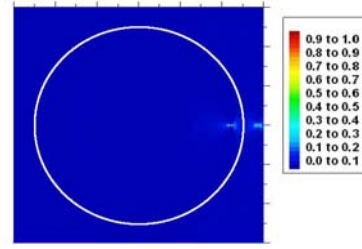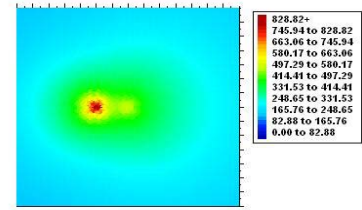
of the scatterer has been greatly modified and some portions of the power have even been shifted beyond the cylinder. It can be explained by that the electrically small cylinder is at resonance and the induced moments cause the shift of the power. A cylinder with DNG material and smaller radius is thus of partiuclar interest as shown in Fig. 8. In order to investigate the resonance effects more clearly, we put the line source closer to the cylinder with a distance of 0.15λ. It is interesting to find that the electric field retained inside the cylinder is much bigger than that of the incidence, and the electric field near the cylinder is also enhanced. This phenomenon is quite potential and distinguished compared to the result of normal DPS cylinder with small radius.

Finally, the real parts of field components, H_ρ and H_ϕ, scattered by a two-layered cylinder filled alternately with DNG and DPS material are shown in Fig. 9and Fig. 10. In this case, a line source is placed at $\rho_0 = 9.5\lambda$ and $\phi_0 = 0$, the radii of two layers are $r_1 = 8\lambda$ and $r_2 = 5\lambda$, respectively. The layer 1 is filled with DNG material $(-\varepsilon_0, -\mu_0)$ and the layer 0 and 2 are filled with (ε_0, μ_0). As we expect, the tangential components H_ϕ is equal on the layered interfaces. Another tangential component of E_z is also continuous across the interfaces. While the normal component H_ρ is not, which satisfies by default the continuity of normal component of magnetic
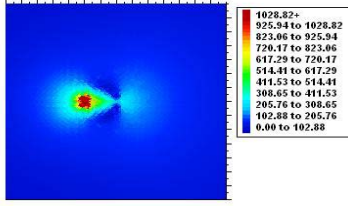
Fig. 7: The amplitude of Poynting power for a one-layered cylinder with $(4\varepsilon_0, \mu_0)$ and $a = 0.05\lambda$.
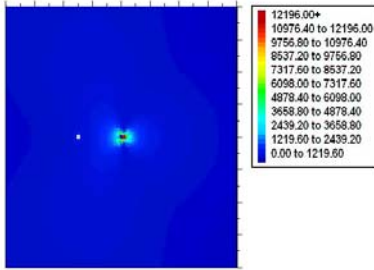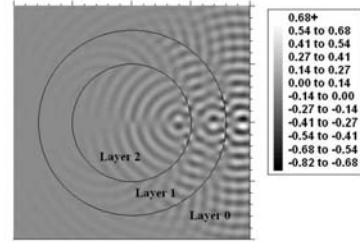

Fig. 9: The real part of H_ρ component of electromagnetic wave propagating through a two-layered cylinder with DNG and DPS materials.

Fig. 8: The amplitude of electric field for a one-layered cylinder with $(-4\varepsilon_0, -\mu_0)$ and $a = 0.01\lambda$.

Fig. 10: The real part of H_ϕ component of electromagnetic wave propagating through a two-layered cylinder with DNG and DPS materials.

flux density $\boldsymbol{B}$ across the interfaces between the DNG and DPS materials.

4. Conclusion

In this paper, we applied the eigenfunction expansion method to generally express the fields in a multilayered cylinder filled by a double negative medium and a double positive medium. The eigenfunction expansion coefficients are determined by enforcing the tangential electric and magnetic field components continuous at the interfaces. The imaging of a line source by this cylinder is observed when the radius $r \gg \lambda$. The electric field and power of those cylinders with small radii, filled with DNG and DPS materials, have been investigated. Moreover, field components for a two-layered cylinder alternately filled with DNG and DPS materials are calculated. The normal component is found to be discontinuous at the boundaries, and the tangential components are not, which agrees, as expected, with the boundary conditions.
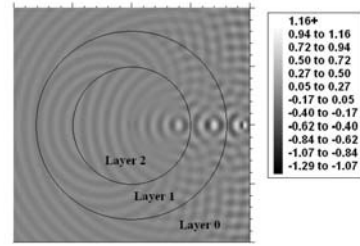
Acknowledgments

References

[1] V. G. Veselago, "The electrodynamics of substances with simultaneously negative values of ε and μ," Soviet Physics Uspekhi, vol. 10, no. 4, pp. 509–514, 1968.

[2] J. B. Pendry, A. J. Holden, D. J. Robbins, and W. J. Stewart, "Magnetism from conductors and enhanced nonlinear phenomena," IEEE Trans. Microwave Theory Tech., vol. 47, no. 11, pp. 2075–2084, November 1999.

[3] D.R. Smith, Willie J. Padilla, D.C. Vier, S.C. Nemat-Nasser, and S. Schultz, "Composite medium with simultaneously negative permeability and permittivity," Physical Review Letters, vol. 84, no. 18, pp. 4184–4187, May 2000.

[4] Y. Zhang, T.M. Grzegorczyk, and J.A. Kong, Propagation of electromagnetic waves in a slab with negative permittivity and negative permeability, vol. 35, EMW Publishing, Cambridge, Boston, 2002.

[5] J. A. Kong, "Electromagnetic wave interaction with stratified negative isotropic media," Progress in Electromagnetics Research, pp. 1–52, 2002, PIER35.

[6] L.W. Li, D. You, M.S. Leong, and T.S. Yeo, Electromagnetic scattering by multilayered chiral-media structures: a scattering-to-radiation transform, vol. 26, EMW Publishing, Cambridge, Boston, 2000.

[7] J.R. Richmond, "Te-wave scattering by a dielectric cylinder of arbitrary cross-section shape," IEEE Trans. Antennas Propagation, vol. 14, no. 4, pp. 460–464, July 1966.

[8] A. J. Ward and J. B. Pendry, "Refraction and geometry in maxwell's equation," Journal of Modern Optics, vol. 43, no. 4, pp. 773–793, 1996.